Flow Around a Pipeline and Its Stability in Subsea Trench

Seungbae Lee*†, Sung-Wook Jang
Department of Mechanical Engineering, Inha University
Chul H. Jo, Sung-Guen Hong
Department of Naval Architecture and Ocean Engineering, Inha University

Offshore subsea pipelines must be stable against external loadings, which are mostly due to waves and currents. To determine the stability of a subsea pipeline on the seabed, the Morrison equation has been applied with prediction of inertia and drag forces. When the pipeline is placed in a trench, the force acting on it is reduced considerably. Therefore, to consider the stability of a pipeline in a trench, one must employ reduction factors. To investigate the stability of various trenches, we numerically simulated flows over various trenches and compared them with experimental data from PIV (Particle Image Velocimetry) measurements. The present results were produced at Reynolds numbers ranging from 6×10^3 to 3×10^5 based on the diameter of the cylinder. Quasi-periodic flow patterns computed by large-eddy simulation were compared with experimental data in terms of mean flow characteristics for typical trench configurations (W/H=1 and H/D=3, 4). The stability for various trench conditions was addressed in terms of mean amplitudes of oscillating lift and drag, and the reduction factor for each case was suggested for pipeline design.

Key Words : Trench, Stability of Pipeline, Large-Eddy Simulation, Particle Image Velocimetry, Drag Reduction Factor

Nomenclature

C_0 : Sound speed
C_D : Drag coefficient
C_{fg} : Cross-correlation coefficient
C_L : Lift coefficient
C_S : Smagorinsky constant
D : Diameter of cylinder
G : Gaussian filter function
H : Depth of trench
Re : Reynolds number
S : Viscous part of the stress tensor
$\overline{S}_{kl}$: Resolved scale strain rate tensor
T_w : Period of oscillatory flow
T : Stress tensor
U_m : Amplitude of oscillatory flow velocity
U_∞ : Free stream velocity
W : Opening length of trench
Δ : Filter size
Ω : Integration domain
δ : Boundary-layer thickness
η : Kolmogorov scale
ν_T : Subgrid-scale eddy viscosity
ρ : Density
$\overline{\sigma}_{kl}$: Filtered viscous stress tensor
τ_{kl} : Subgrid-scale stress tensor
$\sqrt{\overline{x'^2}}$: Root mean square of x

† First Author
* Corresponding Author,
E-mail : sbaelee@inha.ac.kr
TEL : +82-32-860-7325; **FAX** : +82-32-868-1716
Department of Mechanical Engineering, Inha University, 253 Yonghyun-dong, Nam-gu, Inchon 402-751, Korea.(Manuscript **Received** August 18, 2000; **Revised** January 29, 2001)

1. Introduction

The offshore industry has long recognized the importance of subsea pipelines as a link for the transmission of materials between onshore and offshore facilities. Although subsea pipelines are costly to install and maintain, relative to onshore pipelines, they still remain the most feasible and

economical method for transporting materials. To insure their continuous operation, adequate criteria for design must be provided. A lack of necessary information for their design has introduced high safety factors which in turn have increased the construction cost. Information concerning hydrodynamic loads can help to reduce the uncertainty and therefore the overall cost (Knoll and Herbich, 1980).

The correct estimation of external forces on the subsea pipelines has been a topic of considerable interest and discussion. Many experiments have been conducted both in the ocean and in the laboratory for wave and current channels. The test results have frequently shown extreme scatter (Garrison, 1980).

The strategies for dealing with turbulence are many: turbulence models (educated guesses about the needed Reynolds stresses), statistical theory of turbulence (to gain fundamental understanding), and direct numerical simulation. The LES is one of the more promising modes of numerical simulation of turbulence. One of the main differences between the conventional method of RANS (Reynolds-Averaged Navier-Stokes) solver and the LES technique is the averaging process involved. In this study, unsteady, viscous flows over a two-dimensional cylinder in a trench are computed by using the LES technique with Smagorinsky's eddy viscosity model combined with a truncated deductive subgrid-scale model.

The turbulent time-mean flow around a subsea pipeline resting on the ocean bottom is not symmetric; therefore, a non-zero mean lift must exist together with waves (sumer, 1997). There have been numerous studies to develop the criteria to predict the hydrodynamic loads imposed by external waves and currents. The purpose of this research is to investigate the effect of trench slope and depth on the hydrodynamic force acting on a pipeline. Turbulent flow in a trench on which a two-dimensional pipeline model rests was numerically computed and experimentally verified using the PIV technique in a circulating water channel. The reduction in force coefficients due to sheltering effect was obtained and reported for steady current in this study. The characteristics of oscillating lift and drag coefficients, and reduction coefficients for each trench slope can also be applied to estimate the stability of a pipeline with scour process occurring in trench sections.

2. Numerical Simulation

2.1 Governing equations and subgrid-scale modeling

Development of an LES formulation applicable to a non-orthogonal grid system begins with the incompressible continuity, and Navier-Stokes equation in integral form.

$$\int_s \vec{u}\cdot\vec{n}dS=0 \tag{1}$$

$$\frac{\partial}{\partial t}\int_\Omega \rho\vec{u}d\Omega+\int_s \rho\vec{u}\vec{u}\cdot\vec{n}ds = \int_s T\cdot\vec{n}dS+\int_\Omega \rho\vec{b}d\Omega \tag{2}$$

Direct filtering of the continuity equation yields:

$$\frac{\partial\overline{u}_k}{\partial s_k}=0 \tag{3}$$

Direct filtering of the momentum equation yields:

$$\rho\left[\frac{\partial\overline{u}_k}{\partial t}+\frac{\partial}{\partial x_l}(\overline{u}_k\overline{u}_l)\right]=-\frac{\partial\overline{p}}{\partial x_k}+\frac{\partial\overline{\sigma}_{kl}}{\partial x_l}+\frac{\partial\tau_{kl}}{\partial x_l} \tag{4}$$

where $\tau_{kl}=-\rho\left(\overline{\bar{u}_k\bar{u}_l}-\overline{\bar{u}_k}\overline{\bar{u}_l}+\overline{\bar{u}_k\bar{u}'_l}+\overline{\bar{u}_l u'_k}+\overline{u'_k u'_l}\right)$ is called the subgrid-scale stress tensor.

The filtered momentum equation is now solvable if we provide a model for τ_{kl}. The subgrid-scale stress tensor, τ_{kl}, can be decomposed into the subgrid-scale Leonard, cross, and Reynolds stresses based on Gaussian filtering. Smagorinsky (1963) was the first to propose a model for the subgrid-scale stresses. His model assumes that they follow a gradient-diffusion process, similar to molecular motion. It is still the most popular algebraic eddy viscosity model, with τ_{kl} given by

$$\tau_{kl}=2\nu_T\overline{S}_{kl},\quad \nu_T=\overline{\rho}C_s^2\overline{\Delta}^2|\overline{S}| \tag{5}$$

where ν_T is the subgrid eddy viscosity, C_s is the Smagorinsky constant, $\overline{S}_{kl}$ is the resolved scale

strain-rate tensor and $|\overline{S}| = (2\overline{S}_{kl}\overline{S}_{kl})^{1/2}$.

The dynamic subgrid scale turbulence model was proposed by Germano et al. (1991) to simulate the flow state by locally calculating the eddy viscosity coefficient through double filtering. The procedures of Germano et al. were used by Jordan et al. (1998) to derive an expression for Smagorinsky's coefficient in the generalized curvilinear form, and to simulate the near wake of a circular cylinder. This model exhibits the proper asymptotic behavior near the boundaries or in laminar flow without requiring damping or intermittency. However, these models are more demanding computationally due to double filtering at each time step.

To deductively model the Reynolds subgrid-scale stress tensor, τ_{kl}, which is applicable to the incompressible flow with structured grids, we must consider the quantity $\overline{u_k u_l} - \bar{u}_k \bar{u}_l$. Using the Taylor series expansion for Gaussian filtered quantities, we have

$$\overline{u_k u_l} = \bar{u}_k \bar{u}_l + \frac{\Delta^2}{12}\left(\nabla \bar{u}_k \cdot \nabla \bar{u}_l\right) + \frac{1}{2}\left(\frac{\Delta^2}{12}\right)^2 \left(\nabla\nabla \bar{u}_k : \nabla\nabla \bar{u}_l\right) + \cdots \quad (6)$$

In principle, an exact large-eddy simulation would be found by keeping all terms in the expansion for the deductive model. By keeping all terms, all scales down to the Kolmogorov scale η would be accounted for. Although viscosity may be very large, it is finite and responsible for the final energy dissipation of the system. But at large Reynolds numbers, as a practical matter, we cannot deal with the dissipation scale directly. So based on the Kolmogorov hypothesis, we make the reasonable assumption of a dynamic similarity, in a statistical sense, between the smallest eddy dictated by viscosity and the smallest eddy allowed by the filter size Δ which presumably lies within the inertial subrange. From experiments we know that if the Reynolds number is large enough, the inertial subrange begins at about 1/3rd the large scale. This is the Smagorinsky model.

Therefore, the truncated deductive model in Eq. (6) treats the eddies immediately below Δ, but not

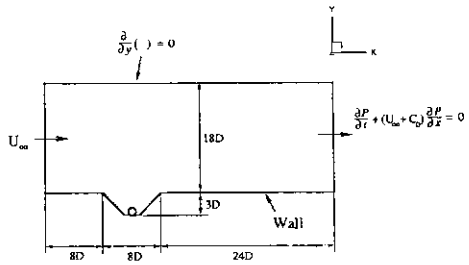

(a) Computational domain of trench with slope of 1.0

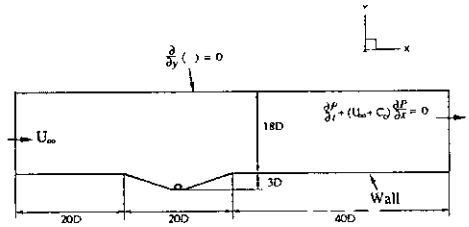

(b) Computational domain of trench with slope of 1/3

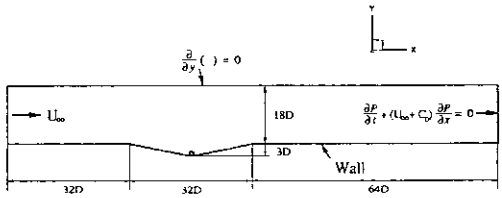

(c) Computational domain of trench with slope of 1/5

Fig. 1 Computational domains of trenches with a cylinder

those very small eddies which account for the dissipations. Thus it seems fair to conclude that we need the Smagorinsky model to describe the dissipation correctly, and the truncated deductive model to ensure a smooth cascade process. A linear combination of deductive model and eddy viscosity model turned out to correlate better with the exact value than Smagorinsky model alone by Lee and Meecham (1996).

2.2 Numerical method and boundary conditions

The numerical simulation of a turbulent flow over a trench with a cylinder resting on it was performed with the modified ANSWER code (Runchal, 1993), which accommodates the subgrid-scale model proposed by Lee (1992) for LES computation.

The equation of continuity was transformed into an equation for computating density in this study. This approach of working directly with the density variable is termed DEFCON for Density Equation Formulation of Continuity equation. The governing Navier-Stokes equations are integrated by Finite Volume Method (FVM) for a collocated, structured grid system. A major advantage of this method is that it intrinsically preserves mass, and material fluxes both on local and global scales.

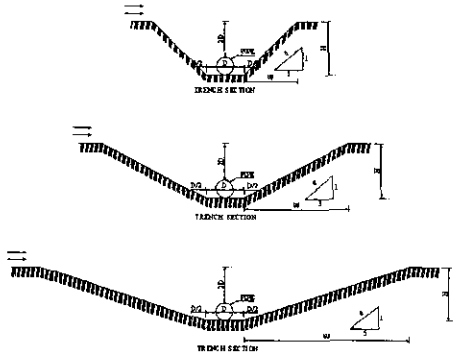

Fig. 2 Schematic diagram of pipe in trench

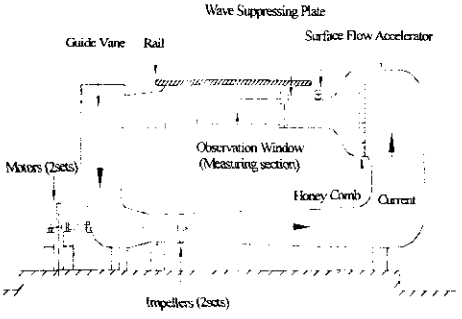

Fig. 3 Schematic of water tunnel

The numerical integration starts with the assumption of an integration profile for the state variable. The CONDIF (Runchal, 1987) scheme, which is stable and second order accurate, is employed in this research (see Runchal(1987)). In this work, the Alternating Direction Implicit (ADI) method was used, which solves the set of algebraic equations in three sweeping directions. This temporal discretization of the ADI method is proven to be unconditionally stable in a linear sense. But it may not be accurate in time if the time step is large due to neglecting the third-order term which is essential to factorization. The details of the formulation have been described by Lee et al. (1999) along with some validation studies.

To numerically simulate turbulent flows in the trenches, H-type grid systems of 141×67, 150×67, and 160×67 (in x and y directions) were used with the inflow and outflow boundaries placed at 8D and 24D, 20D and 40D, 32D and 64D for the cases of $W/H=1.0$, 3.0, and 5.0, respectively (see Fig. 1). As an exit boundary condition, the simplified convective one among non-reflecting boundary conditions was also employed (Hayder and Turkel, 1995).

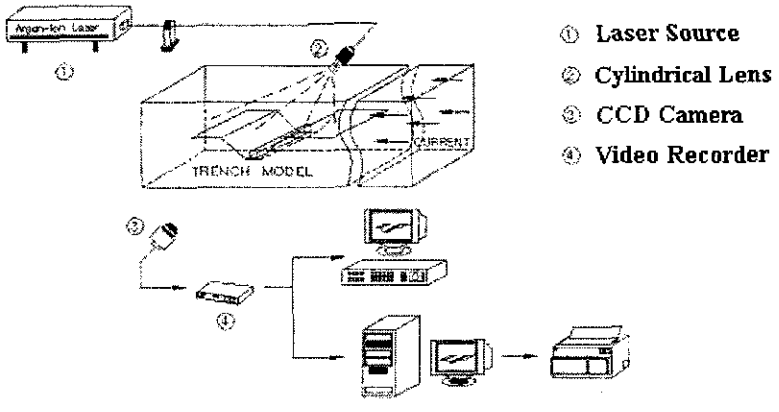

Fig. 4 Experimental setup for P.I.V. measurement

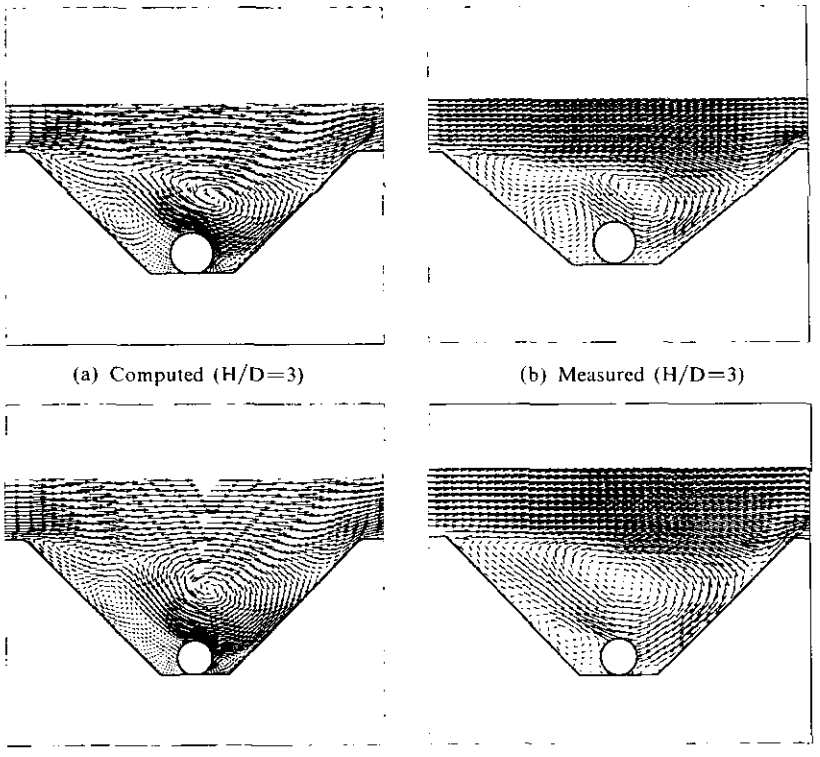

(a) Computed (H/D=3) (b) Measured (H/D=3)

(c) Computed (H/D=4) (d) Measured (H/D=4)

Fig. 5 Computed mean-velocity patterns ((a), (c)) compared with measured ones ((b), (d)); (a) and (b) for H/D=3; (c) and (d) for H/D=4 with $Re_D=6\times10^3$ and $\delta/H=0.1$ fixed

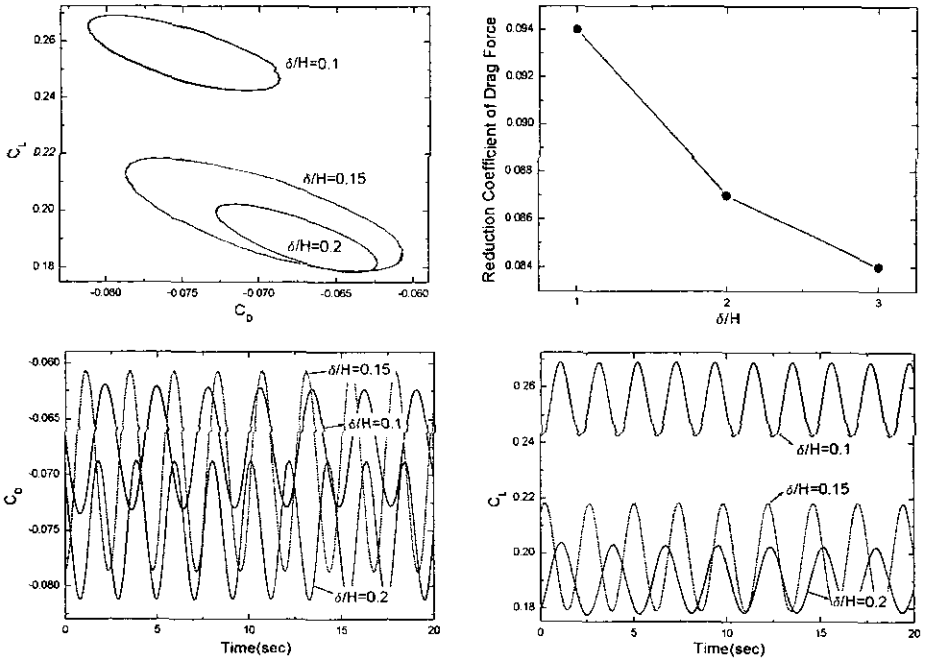

Fig. 6 Effects of boundary layer thicknesses on drag reduction coefficients, and C_D-C_L characteristics for H/D=3, W/H=1, and $Re_D=6\times10^3$

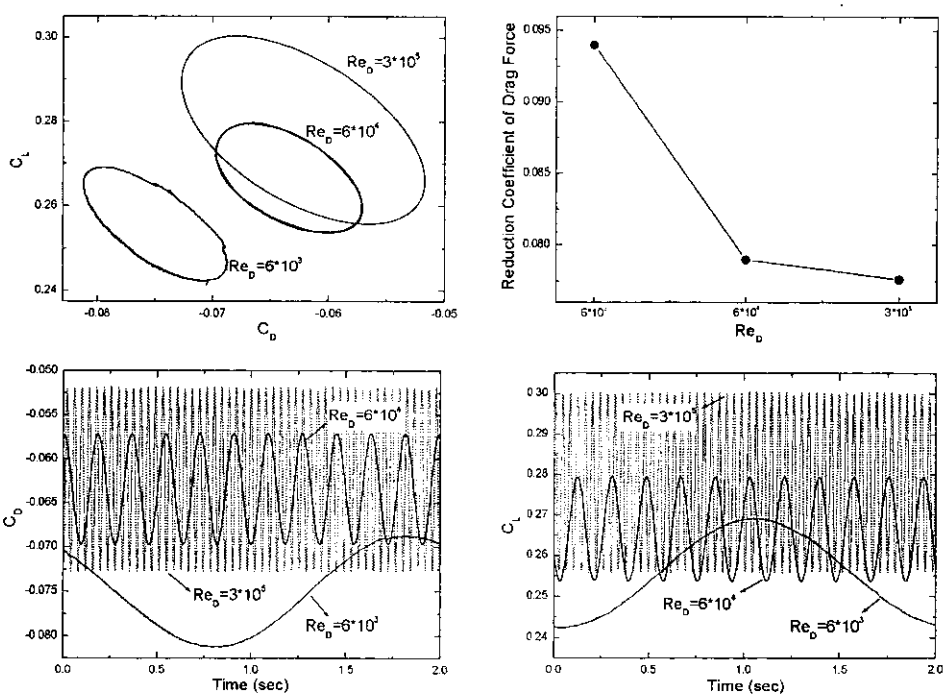

Fig. 7 Effects of Reynolds numbers on drag reduction coefficients, and C_D-C_L characteristics for $\delta/H=0.1$, $H/D=3$, $W/H=1$

3. Experimental Measurements

3.1 Experimental setup

A schematic diagram of a pipeline in a trench is shown in Fig. 2 in which D and H stand for outside diameter of pipeline and cover or burial depth, respectively. The trench slope is represented as "a" as indicated in Fig. 2. The frame for the trench section was made out of bronze, and the seabed of transparent flexi-glass of 5 mm thickness. The investigation was conducted in a low-speed (0.15~1.7 m/s), circulating water tunnel as shown in Fig. 3. The test section of the water tunnel is 3.5 m long, and has a cross section of 1.2 m (width)×0.9 m (height) and water depth of 0.7 m. A wave suppressing plate is located upstream of the test section to minimize free surface effect. The turbulent intensity of the test section was less than ±2.0% and the uniformity of steady current was found to be within ±1.5% at a velocity of 1.0 m/s. To provide a uniform inlet flow, a flat-plate was attached in front of the trench model. The leading edge of the flat-plate was rounded so as not to introduce any separation near the edge. To minimize side-wall effects, the model was installed 15 cm apart from the wall, which made the width to diameter ratio to be about 30. Placing the measuring plane at the center of the model minimized the side-wall effect. The model, which was set up 30 cm above the tank bottom, was securely fastened by two support piles downstream, and was free of any vibration effect. The upstream steel support was provided right behind and below the model so as not to have any turbulence effect on the trench.

3.2 P.I. V. Measurements

To identify velocity fields in the trench with various slopes, P.I.V. measurements were performed with an optical setup shown in Fig. 4. To provide the trench with two-dimensional sheet of light in the symmetric plane, a 1.0W Ar-ion laser was supplied to the flow field through a fiber optic cable together with a cylindrical lens. The particles of 150-200 μm diameter having about

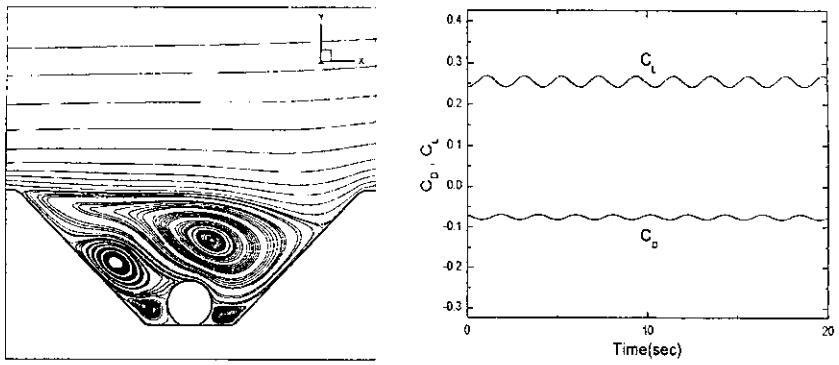

(a) W/H=1.0

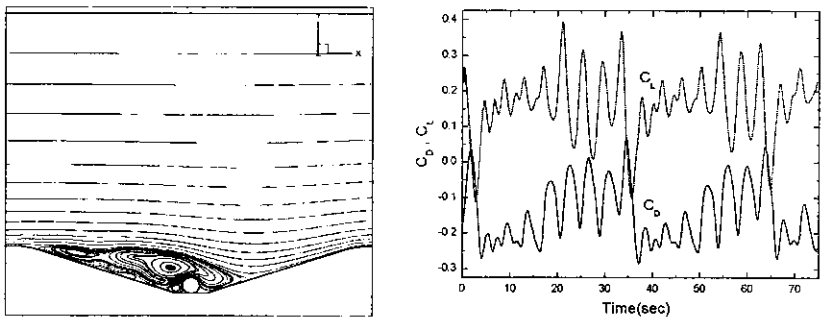

(b) W/H=3.0

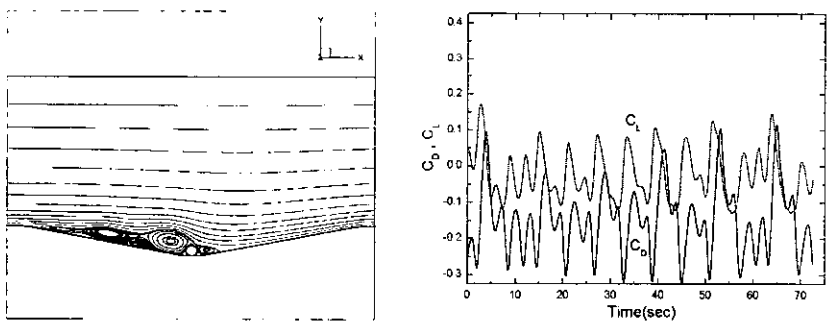

(c) W/H=5.0

Fig. 8 Mean-streamline patterns and unsteady C_D-C_L characteristics for each W/H with H/D=3, δ/H=0.1, and $Re_D=6\times10^3$ fixed

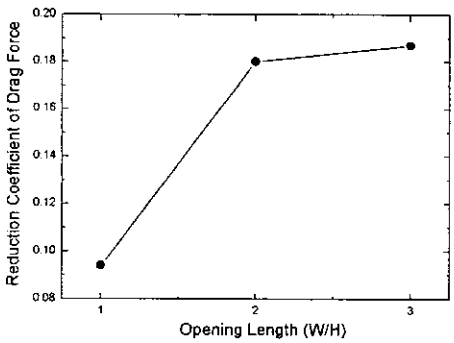

Fig. 9 Drag reduction coefficients vs. opening length (H/D=3.0, δ/H=0.1, and $Re_D=6\times10^3$)

same density with water were seeded in the tunnel after static electricity was suppressed.

The visual image was captured by a Charge Coupled Device (CCD) camera (SONY-XC77RR) and stored on a tape via a video recorder. The captured images controlled by AOM were sent to odd and even fields and processed by an image board (DT3155, 640×480 pixels) on a host computer (250MHz CPU). After the removal of background noise and the compensation of rotation, the searching area was set to have a radius of 25 pixels with correlation area

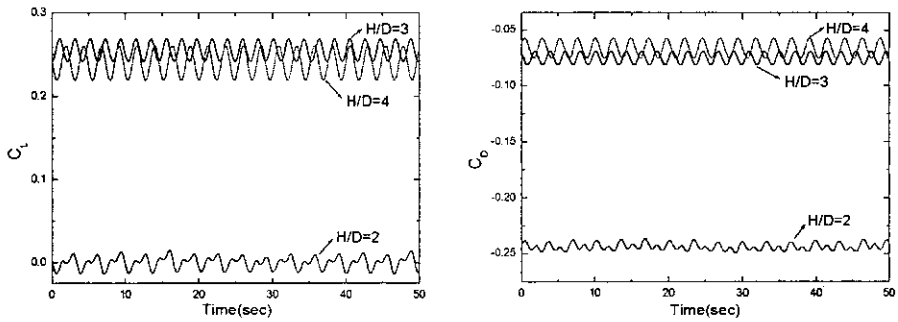

Fig. 10 Effects of cover depth ratio on C_D-C_L characteristics (W/H=1.0, δ/H=0.1, and Re_D= 6×10^3)

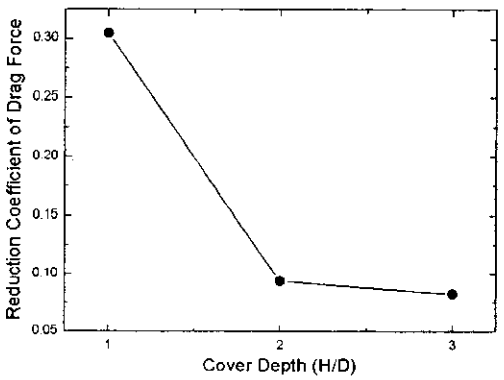

Fig. 11 Drag reduction coefficients vs. cover depth ratios(W/H=1.0, δ/H=0.1, and Re_D=6×10^3)

radius of 30 pixels. Optimized searching of cross-correlation coefficients was conducted to determine the velocity vectors by using Eq. (7) (Raffel, et.al, 1997).

$$C_{fg}=\frac{\sum_{i=1}^{n^2}(f_i-\bar{f}_i)(g_i-\bar{g}_i)}{\sqrt{\sum_{i=1}^{n^2}(f_i-\bar{f}_i)^2\sum_{i=1}^{n^2}(g_i-\bar{g}_i)^2}} \quad (7)$$

4. Results and Discussion

The wake flow behind a circular cylinder has been considered as a fundamental study about the wake of a bluff body of arbitrary shape. This problem, which is called Strouhal shedding or Kármán vortex, has many engineering applications in flows around rows of tubes in heat exchangers or marine structures.

A 2D simulation of a circular cylinder in a free-stream is known to under-predict the formation length of the primary vortex while over-predicting the strength and the shedding frequency. However, vortex shedding may be suppressed for a cylinder near a wall. Spanwise structures are also assumed not to modify the characteristic flow patterns in the trench considerably.

The mean flow around a near-wall cylinder is not symmetric; therefore, a non-zero mean lift must exist. When the cylindrical pipeline is placed in a trench hole, the forces are reduced considerably. Both the drag and the lift forces are reduced by a factor 5 to 10, depending on the position of the pipe in the trench hole. This is due to the sheltering effect by the trench. It was reported that in the case of a same sized trench hole but with a steeper slope, the reductions in the forces are much larger.

Even though the incoming flow is steady, the cylinder in the trench may experience an oscillatory flow, and an additional parameter called Keulegan-Carpenter (KC) number should be considered. It is defined by $KC=U_mT_w/D$. When KC is small, separation behind the cylinder in the free stream may not occur even at high Reynolds numbers (Sumer, 1997).

The trenches considered in this study may be classified as open cavities because a shear layer separated from the corner of the backward facing slope hits on the other side of the forward facing slope (Tracy and Plentovich, 1997). Therefore, oscillatory behavior of lift and drag forces is

observed even in a steady current. A cylinder placed on the sea bottom would feel the approaching flow turbulence that is generated within the bottom boundary layer. In the case of a cylinder in a trench, external turbulence acts on the cylinder indirectly via oscillatory motion. The boundary layer approaching the trench was assumed to be laminar in this study and the flows may become turbulent in the trench.

The parameters of geometrical importance may be listed as the boundary layer thickness (δ), the opening length (W), the depth of trench (H), and the cylinder diameter (D). Therefore, three non-dimensional parameters δ/H, H/D, and W/H are formed. The non-dimensional numbers of dynamic importance in this study are the Reynolds (Re) and Keulegan-Carpenter (K-C) numbers.

The effect of incoming boundary-layer thickness on oscillatory motions in the trench was numerically studied for the cases of δ/H=0.1, 0.15, and 0.2 with H/D=2.0, W/H=1.0, and Re_D=6×10^3. To figure out the Reynolds number effect on the lift and drag, the case of $Re_D=6\times10^3$, which is the same condition as experimental measurement, and the cases of 6×10^4 and 3×10^5 were implemented in the numerical tests. To estimate the stability of a pipe for each configuration, numerical tests were conducted for the cases of H/D=2, 3, 4, and W/H=1, 3, 5 at the $Re_D=6\times10^3$ and δ/D=0.1.

4.1 Mean flow patterns in open trench

The computed and measured velocity vectors are compared for H/D=3 and 4 with $Re_D=6\times10^3$ and δ/H=0.1 in Fig. 5. The separated shear-layer in the fore part of the trench produces several vortex motions, and the primary vortex induces reverse flow over the cylinder. This jet-like flow interacting with the separated shear-layer creates oscillatory motions in the trench.

4.2 Force coefficients for pipelines in open trench

The drag reduction coefficient is defined as the drag force on a cylinder in an open trench divided by the drag force on a cylinder on sea bottom.

The phase characteristics between C_D and C_L are depicted, along with drag reduction factors, in Fig. 6 for different incoming boundary layer thicknesses. As the boundary-layer thickness increases, both the mean lift and drag coefficients tend to decrease continuously in the absolute sense for the steepest trench among the types considered (H/D=3, $Re_D=6\times10^3$).

In Fig. 7, the dependence of drag reduction coefficient and C_D-C_L characteristics on Reynolds number can be found. As the Reynolds number increases, the mean lift coefficients increase, while the mean drag coefficient decreases in the absolute sense for the case of δ/H=0.1, H/D=3, and W/H=1. The K-C numbers are found to be approximatly 12.0 for the range of Reynolds numbers considered.

The mean flow patterns and time histories of C_D and C_L are compared for different opening lengths with the trench depth ratio, incoming boundary-layer thickness ratio, and Reynolds number fixed as 3.0, 0.1, and 6×10^3, respectively (see Fig. 8). The oscillating amplitudes of lift coefficient for the case of W/H=3.0 are found to be greater than those for the widest opening case of W/H=5.0, due to the unsteady nature of separated shear-layer when W/H is equal to 3.0, which means more susceptibility to external disturbances. The drag reduction coefficients become greater as the trench slope decreases, as shown in Fig. 9. Figures 10 and 11 also indicate that the reduction factor decreases as the cover depth increases for the case of W/H=1.0, δ/H=0.1, and $Re_D=6\times10^3$.

5. Conclusions

The reduction factors for various trench slopes and cover depths at three Reynolds numbers were investigated numerically and experimentally. From the numerical/experimental results, the following are observed:

(1) As the trench slope and the cover depth ratio (H/D) increase, the reduction factors decrease. Less scouring is expected.

(2) The external forces acting on the cylinder get reduced as the laminar incoming boundary-

layer thickness increases, and the oscillating lift forces are sensitive to the Reynolds number with the K-C numbers kept nearly constant at around 12.0 for the steepest case.

(3) The opening length ratio (W/H) is the dominant parameter for determining the mean drag force on a cylinder in the trench, while the cover depth ratio (H/D) the dominant influence on the mean lift forces on the cylinder.

These oscillating drag/lift characteristics and reduction factors obtained in this study could improve hydrodynamic loading estimation and reduce subsea pipeline construction cost.

References

Knolll, D.A., Herbich, J.B., 1980, "Wave and Current Forces on a Submerged Offshore Pipeline," *Offshore Technology Conference*, pp. 227~234.

Garrison, C.J., 1980, "A Review of Drag and Inertia Forces on Circular Cylinders," *Offshore Technology Conference*, pp. 205~218.

Sumer, B.M., 1997, *Hydrodynamics Around Circular Structures*, Advanced Series on Ocean Engineering-Vol. 12, World Scientific

Smagorinsky, J., 1963, "General Circulation Experiments with the Primitive Equations, Part I : the Basic Experiment," *Monthly Weather Rev.*, Vol. 91, pp. 99~164.

Germano, M., Piomelli, U., Moin, P. and Cabot, W. H., 1990, "A Dynamic Subgrid-Scale Eddy Viscosity Model," *Physics of Fluids A.*, Vol. 3, pp. 1760~1765.

Jordan, S.A., Ragab, S.A., 1998, "A Large-Eddy Simulation of the Near Wake of a Circular Cylinder," *J. of Fluids Eng.*, Vol. 120, pp. 243~252.

Lee, S., Meecham, W.C., 1996, "Computation of Noise from Homogeneous Turbulence and a Free Jet," *Int'l J. Acoust. and Vib.*, Vol. 1, pp. 35~47.

Runchal, A.K., Bhatia, S.K., 1993, "ASME Benchmark Study: ANSWER Predictions for Backward Facing Step and Lid-driven Cubical Cavity," *ASME*, FED-Vol. 160, pp. 43~54.

Runchal, A.K., 1987, "CONDIF: A Modified Central-Difference Scheme for Convective Flows," *Int'l J. Num. Methods in Eng.*, Vol. 24, pp. 1593~1608.

Lee, S., Runchal, A.K., Han, J.-O., 1999, "Subgrid-scale Model in Large-Eddy Simulation and Its Application to Flow about Yawed Cylinder and Cavity Flows," *3rd ASME/JSME Joints Fluids Eng. Conf.*, San Francisco

Hayder, M.E., Turkel, E., 1995, "Nonreflecting Boundary Conditions for Jet Flow Computations," *AIAA J.*, Vol. 33, No. 12, pp. 2264~2270.

Raffel, M., Willert, C.E. and Kompenhans, J., 1998, *Particle Image Velocimetry*, Springer

Tracy, M.B., Plentovich, E. B., 1997, "Cavity Unsteady-Pressure Measurements at Subsonic and Transonic Speeds," NASA Technical Paper, 3669